RSC Sustainability

ROYAL SOCIETY OF CHEMISTRY

CRITICAL REVIEW

View Article Online
View Journal

Cite this: DOI: 10.1039/d5su00397k

Toward stable operation for thermochemical conversion of biomass and waste: ash chemistry for understanding ash adhesion at high temperatures

Genki Horiguchi[b] and Yohei Okada *[a]

Toward the stable and efficient thermochemical conversion of coal, biomass and waste, the handling of ash particles derived from the unburnable portion of fuels is a key issue because ash can cause operational problems as a result of its adhesion characteristics at high temperatures. Understanding the relationship between ash chemistry and adhesion characteristics is a major focus in this research field. To investigate the relationship between the chemical properties of materials and their function, an approach using materials with well-designed chemical compositions is effective. However, real ash generated from commercial plants has complicated chemical properties. In this review, we highlight studies using synthetic ash, which is experimentally prepared from commercially available chemicals, to understand the relationship between ash chemistry and adhesion. Synthetic ash with simplified and carefully designed chemical components is helpful for attaining a mechanistic understanding of the influence of ash chemistry on adhesion.

Received 3rd June 2025
Accepted 16th December 2025

DOI: 10.1039/d5su00397k

rsc.li/rscsus

Sustainability spotlight

Using biomass and wastes instead of fossil fuels is a promising approach because of their high abundance and availability. Thermochemical conversion, combustion and gasification are typical examples of effective methods to utilise the energy of biomass and waste. Toward the stable and efficient thermochemical conversion, the handling of ash particles derived from the unburnable portion of fuels is a key issue because ash can cause operational problems as a result of its adhesion characteristics at high temperatures. Understanding the relationship between ash chemistry and adhesion characteristics is a major focus in this research field. In this review, we highlight studies using synthetic ash, which is experimentally prepared from commercially available chemicals, to understand the relationship between ash chemistry and adhesion.

Introduction

Suppressing the use of fossil fuels, coal and petroleum is a typical example of a key strategy for achieving a sustainable society. Using biomass and wastes instead of fossil fuels is a promising approach because of their high abundance and availability. Thermochemical conversion, combustion and gasification are typical examples of effective methods to utilise the energy of biomass and waste. Thermochemical conversion can produce a large amount of energy, which can be used to produce power.[1] Gasification can also produce syngas, which is a mixture of hydrogen and carbon monoxide and can be used to produce chemicals and synthetic fuels.[2] The development of processes that maximise these advantages in the thermochemical conversion of biomass and waste is required.

The thermochemical conversion of biomass and waste is complicated, and studies on the process span broad topics, such as investigations of reaction mechanisms, furnace and process design and catalytic gasification.[3] The investigation of ash-related phenomena is a topic of interest in this research field.[4] Ash is derived from the unburnable portion of coal, biomass and waste. Particulate ash is produced during thermochemical conversion processes, and the ash plays an important role in various steps of these processes. Ash components have been found to act as catalysts for gasification reactions.[5] In addition, valuable materials such as phosphoric acid can be produced from ash and useful components such as phosphorous can be extracted from ash.[6]

Among the various well-known properties of ash, ash adhesion behaviour is the focus of the present review. Ash particles exhibit high adhesion at high temperatures such as the operating temperatures of commercial plants (600–1000 °C), causing serious problems in plant operation.[7] Ash adhered to heat exchangers adversely affects the heat transfer efficiency, and large aggregates of ash (clinker) can clog ducts.[7] Ash also adheres to the bed materials in fluidised beds, increasing the

[a]Department of Applied Biological Science, Tokyo University of Agriculture and Technology, 3-5-8 Saiwai-cho, Fuchu, Tokyo 183-8509, Japan. E-mail: y.okada@cc.tuat.ac.jp

[b]Energy Catalyst Technology Research Group, Energy Process Research Institute (EPRI), National Institute of Advanced Industrial Science and Technology (AIST), 16-1 Onogawa, Tsukuba, Ibaraki 305-8569, Japan

apparent size of the bed material and stopping fluidisation.[8] Because these events lead to inefficient and unstable plant operation, ash adhesion should be controlled. Irrespective of the adhesion phenomenon, ash-related behaviours are strongly influenced by the chemical properties of the ash. That is, understanding ash chemistry is important for understanding ash-related problems.

The use of well-designed materials is advantageous for understanding the effect of chemical characteristics on material properties and functions. For example, catalysts with various chemical compositions have been designed and prepared and the relationship between their catalytic performance and composition has been discussed.[9] As a result, the mechanisms of catalytic processes can be investigated and applied to catalyst development and industrialisation. Unfortunately, the ash produced from commercial thermochemical plants includes a wide variety of elements (components), and the composition of the ash cannot be experimentally controlled.[10] The unique characteristics of ash make understanding its chemistry difficult (Fig. 1(a) and Table 1). The use of appropriate analytical techniques enables the experimental observation and evaluation of the unique behaviours of ash produced from commercial plants, referred to as 'real ash', and contributes to our understanding of the behaviours that occur in commercial plants. However, understanding the influence of the chemical characteristics of real ash is still challenging and a topic of interest. The use of well-designed and experimentally synthesised compounds contributes to understanding of the relationship between chemical properties and ash behaviour. That is, ash simulants are designed and synthesised and the behaviour of the synthesised ash is evaluated. Specifically, ash-modified materials are designed and synthesised and the behaviours of the synthesised ash are evaluated (Fig. 1(b) and Table 1). As a result, the effect of chemical characteristics on the unique behaviour of the ash can be understood. The compounds that simulate ash are called 'synthetic ash' and are currently being used to study ash chemistry. As expected, studies that use synthetic ashes have helped elucidate detailed mechanisms of ash behaviours. Mechanistic insights obtained from synthetic ash can contribute to our understanding of the behaviour of real ash. This understanding will, in turn, enable appropriate understanding of the large number of complex datasets associated with real ashes and will contribute to the development of methods for predicting ash behaviour at high temperatures when used in combination with advanced tools such as artificial intelligence and data-driven analysis.

This review surveys recent studies in which synthetic ashes were used to understand ash adhesion on the basis of ash chemistry. In particular, this review focuses on studies published since 2013 on synthetic ashes modifying coal, biomass and sewage–sludge ashes. The insights obtained through the long history of coal utilisation have contributed to the use of biomass, sewage sludge and waste, which are the main focus as alternative resources to fossil fuels. This trend is no exception in the study of ash and is addressed in this review. Sewage sludge is not only a potential feedstock for energy and chemical production but also a potential phosphorous resource, and this review focuses on sewage–sludge ash.[6] Before introducing synthetic ash, we discuss some important insights and limitations derived from the analysis of real ashes. The potential applications of synthetic ashes for mechanistic understanding of ash chemistry are presented.

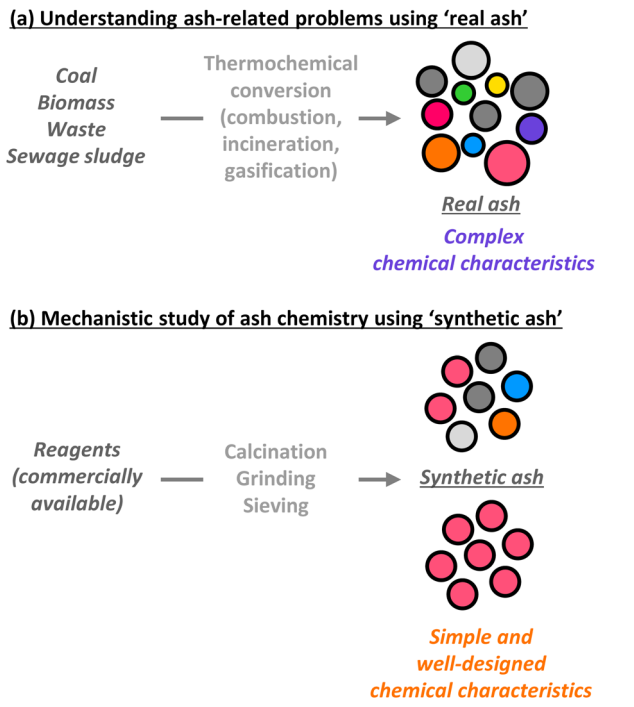

Fig. 1 Comparison of studies using real and synthetic ash.

Chemical composition of ash

Numerous types of real ashes produced from commercial plants have been characterised. The major elements in ash are Na, Mg, Al, Si, P, S, Cl, K, Ca and Fe.[10] Trace amounts of other elements such as heavy metals are also present. Investigating the role of heavy metals in ashes is important for understanding ash behaviour (including corrosion) and the disposal and recycling of heavy metals; their role has been discussed in detail in other advanced reviews.[7c,11]

The chemical characteristics of ash usually depend on the type of fuel.[10,12] In general, coal ashes tend to contain large amounts of Si and Al.[12a] Biomass ashes can contain greater amounts of Ca, K and P than coal ash because these elements are essential for life.[12a] A remarkable characteristic of sewage–sludge ashes, which are produced by wastewater treatment, is the presence of P.[12b] Because removing P from wastewater is important for preserving the aquatic environment, the P in wastewater is concentrated in sewage sludge during the treatment process.[13] Biomass and waste ashes can contain Cl, which promotes corrosion.[14] The presence of ash with a high Ca content has also been reported.[10e,15] As an example, the composition of the ashes previously analysed by our group is shown in Fig. 2.[16] The results are in approximate agreement with the aforementioned trend. The characteristics of ashes

Table 1 Comparison of real and synthetic ashes

	Real ash	Synthetic ash
Origin (precursor)	Coal, biomass, waste and sewage sludge	Commercially available reagents
Chemical characteristic	× Complex	✓ Well-designed and experimentally synthesised compounds
	× Composition cannot be experimentally controlled	
Points	✓ Contributes to understanding the behaviour that occurs in commercial plants	✓ Contributes to understanding the relationship between chemical properties and ash behaviour
	× Difficult to understand the ash chemistry	

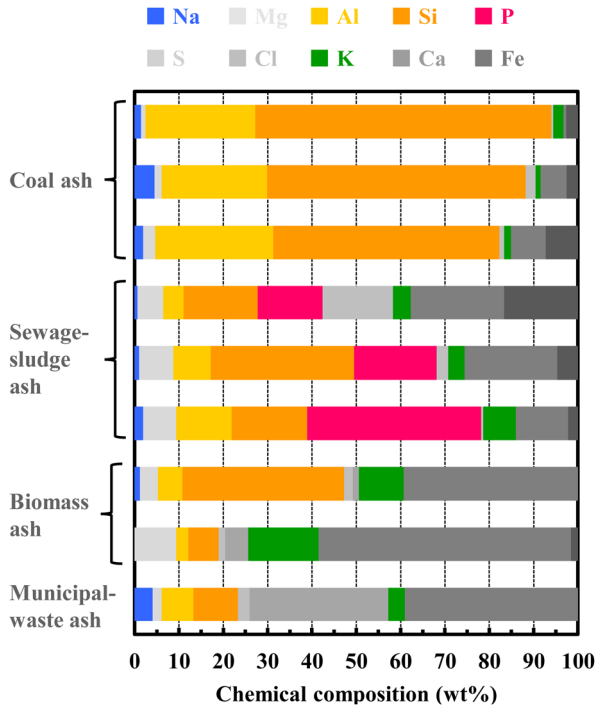

Fig. 2 Chemical compositions of real ashes used in previous studies.[16]

produced from commercial plants are highly variable. Notably, the chemical characteristics are also influenced by the locality of coal, the origin of the biomass (type of wood) and the origin of waste (municipal or industrial).[10] A comprehensive understanding of ash chemistry is important for addressing the diversity of not only coal but also biomass. Various combustion ashes are currently being studied. The authors of previous advanced reviews have discussed the diversity of the chemical characteristics as a result of regional differences and other factors.[10,12,14a]

We also introduce methods for analysing the chemical characteristics of ash. Ash is characterised using common analytical techniques (*e.g.*, X-ray diffraction (XRD), X-ray fluorescence (XRF) spectroscopy, Fourier transform infrared (FT-IR) spectroscopy and scanning electron microscopy with energy-dispersive X-ray spectroscopy (SEM/EDS)) and thermodynamic calculations. Because of the complex chemical composition of ash, interpreting the analytical data is not straightforward. Thermodynamic calculations are useful for estimating stable phases in the ash.[17] In the analysis of real ashes, the distribution of chemical components is an important consideration because of their complex chemical compositions. To evaluate the distribution of chemical composition in ash samples, special techniques such as computer-controlled SEM/EDS (CC-SEM/EDS) are useful.[18]

Ash adhesion at high temperatures: mechanism and quantification

Ash adhesion is generally related to the liquid phase.[19] The liquid phase can form bridges between particles or between a particle and a wall, resulting in liquid bridge force, which is an attraction force. When the liquid phase is present on the surface of particles, the liquid bridge force is stronger than the van der Waals force, which is an attraction force that acts with and without the liquid phase.[20] Therefore, when the liquid phase is present, attention should be paid to the liquid bridging forces. Under high-temperature conditions (500–1000 °C), a liquid phase can form in ash particles.[16e,21] This liquid phase is considered to form *via* the partial melting of ash and the condensation of gaseous components onto the ash particles (Fig. 3(a)).[7c,22] Under certain conditions, the melting temperature of a compound is uniquely determined. However, defining the melting point of ash is difficult because real ashes contain various compounds. As the temperature of the ash is increased, the compound with the lowest melting point among the compounds that compose the ash begins to melt. In addition, ash is a mixture of various components and eutectic mixtures can form. The temperature at which the mixture starts to form a liquid phase is lower than the temperatures at which the single components form a liquid phase because of the formation of a eutectic.[23] Therefore, we note that the liquid phase can be formed below the melting point of the pure components. In addition, the gaseous components of the ash condense onto the particulate ash and/or bed materials in the fluidised-bed process, resulting in the formation of a liquid phase on the surface of these particles.[22] The condensation proceeds because of a decrease in the gas temperature in the plants.[22] These mechanisms result in the formation of the liquid phase under high temperatures, such as those inside thermochemical plants. On the basis of this mechanism, the formation behaviour of the liquid (slag) phase provides useful information for evaluating adhesion at high temperatures. The formation behaviour of the slag phase can be estimated using thermodynamic calculations. The Na, K and P in the ash cause the

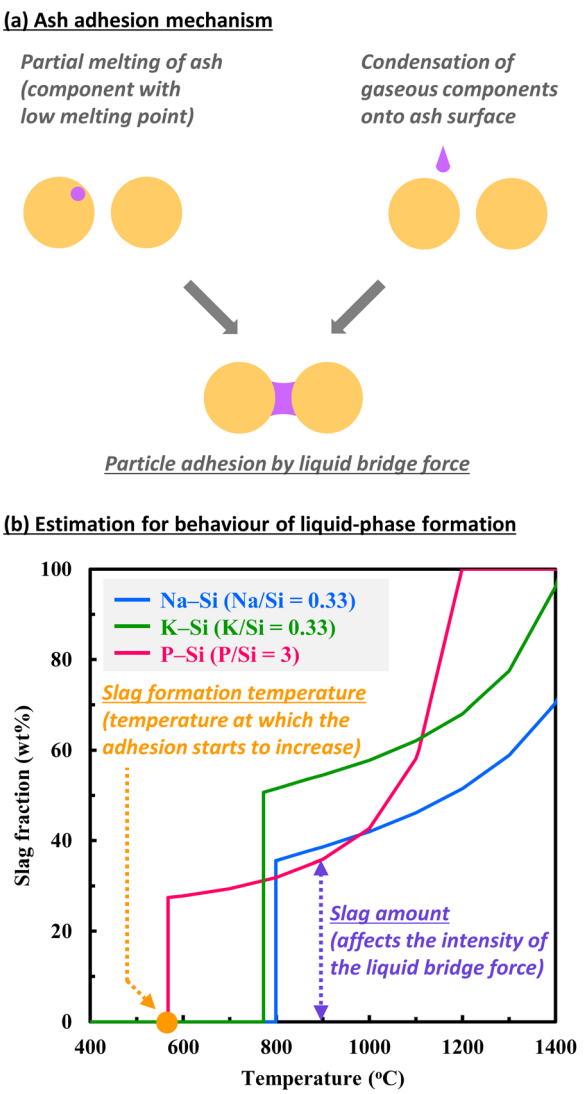

Fig. 3 (a) Schematic of the ash adhesion mechanism under high temperatures and (b) thermodynamic calculations for predicting adhesion. Calculation data were obtained using the FactSage software.

formation of a liquid phase at the operating temperatures of the thermochemical conversion process.[7c,24] As an example, the formation behaviour of the slag phase caused by the interaction of these elements with Si was estimated by thermodynamic calculations (Fig. 3(b)). The important factors obtained from the calculations in evaluating ash adhesion are slag formation temperature and slag amount. The slag formation temperature is the temperature at which the slag phase starts to form as the temperature is increased. Above this temperature, particle adhesion is expected to increase, and attention should be paid to ash adhesion. In addition, the slag amount affects the intensity of the liquid bridge force. The liquid bridge force has been reported to increase with increasing liquid volume.[16a,25] The slag amount is an important factor in predicting the severity of ash adhesion. Interestingly, the formation behaviour of the slag phase is related to the type of element, which indicates that ash chemistry strongly influences ash adhesion behaviour.

Herein, the slag formation temperature—specifically, the melting point—is explained in greater detail. The melting points of the components that can be present in ash are listed in Table 2. The eutectic temperatures of the system that can form in ash are shown in Table 3. The Na-, K- and P-containing ashes can melt at temperatures in the operating temperature range of thermochemical conversion (600–1000 °C). In the fluidised bed systems, the interaction between the ash and bed materials such as SiO_2 warrants attention.[26] The reaction causes the formation of low-melting compounds. In addition, a eutectic mixture can be formed because of the interaction of SiO_2 derived from the bed material with components derived from the ash.[26]

These mechanisms indicate that the chemical compositions of ash influence its adhesion at high temperatures. As mentioned in the previous section, the chemical characteristics of ashes vary and depend on the types of fuels and the origin of the biomass or waste. Therefore, the degree of ash adhesion is strongly influenced by the types of biomasses and wastes because of differences and variations in their chemical characteristics.[12a] Predicting the adhesion degree on the basis of the chemical characteristics of the ash can be useful in developing a method for controlling ash adhesion preliminarily.

Predicting ash adhesion requires understanding the relationship between the chemical composition of ash and its adhesion properties. As a first step toward achieving this objective, the chemical characteristics and adhesion properties of ash should be determined accurately and reproducibly. Although the chemical characteristics of ash are complex, they can be determined using general chemical analysis techniques such as XRD. By contrast, determining adhesion is challenging because measuring the forces acting on microsized particles at high temperatures is difficult.[27] Therefore, the development of methods to quantify ash adhesion is an important topic in this research field.

With respect to the adhesion mechanism, the melting behaviour of ash can be used to evaluate ash adhesion. The fusion temperature of ash is a commonly used index for evaluating ash adhesion at high temperatures.[17a,28] Although this method does not directly measure force, it offers an indication of adhesion based on the aforementioned adhesion mechanism. Specifically, a lower ash fusion temperature (AFT) indicates higher adhesion. AFTs are measured by observation of the

Table 2 Melting point of compounds that can be present in real ash

	Compound	Melting point[a] (°C)
Low melting point	$Na_2Si_2O_5$	875
	$K_2Si_4O_9$	771
	KCl	776
High melting point	Quartz (SiO_2)	1650
	Mullite ($Al_6Si_2O_{13}$)	1850
	$KAlSiO_4$	1690

[a] Obtained from the database of the FactSage software.

Table 3 Eutectic temperatures of the system that can form in real ash

System	Eutectic temperature[a] (°C)
Na_2O–SiO_2	799
K_2O–SiO_2	579
P_2O_5–SiO_2	567

[a] Calculated using the FactSage software.

change in shape and height of a moulded ash specimen with increasing temperature (Fig. 4(a)). The AFT can be defined different ways depending on the extent of the change in shape and height; the initial deformation temperature and fluid temperature are typical examples.[29] Also, to understand the interactions between ash and a metal surface, adhesion demonstrations are experimentally performed using simulated deposition structures, which are ash deposits placed on a metal surface (Fig. 4(b)).[30] Such experiments can simulate real adhesion phenomena but cannot quantify the adhesion.

To quantify the adhesion force of particulate materials, measuring the strength of powder beds, which are formed by packing particles, is a promising method.[27] Strength measurements by tensile and shear tests of powder beds have contributed to our understanding of the mechanical properties of particulate materials and have also been used to study ash adhesion (Fig. 5).[27b,c,31] Ash powder beds prepared experimentally can simulate the adhesion layers of ash formed inside plants. Therefore, quantifying the strength of ash powder beds is important for understanding the mechanical properties of ash adhesion layers. For example, it can be used to predict the growth process of an adhesion layer and to evaluate the external force required to remove an adhesion layer. Other important information obtained from strength measurements includes the adhesion force, F, between particles, which can be determined on the basis of Rumpf theory using the tensile strength of the powder bed, σ:[32]

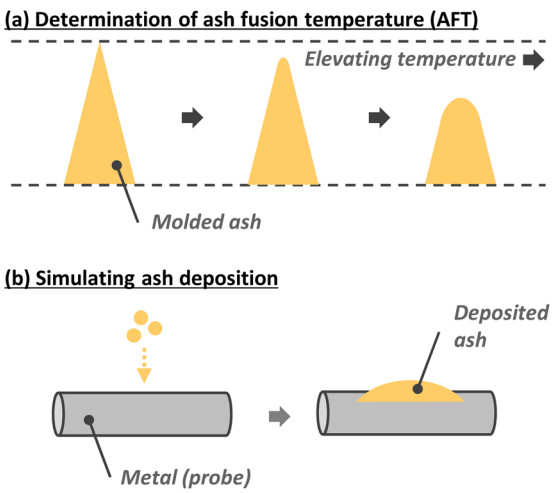

Fig. 4 Typical methods for evaluating ash adhesion at high temperatures. (a) Determining the ash fusion temperature (AFT) and (b) simulating ash deposition.

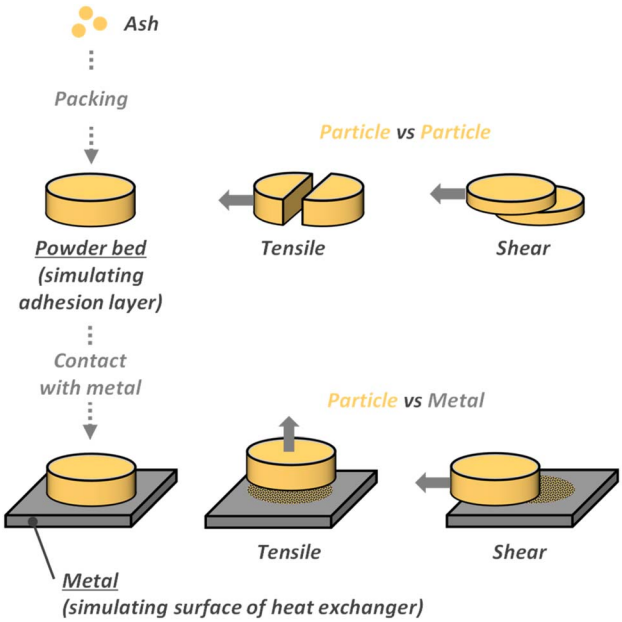

Fig. 5 Evaluating ash adhesion by measuring the strength of ash powder beds.

$$\sigma = \frac{(1-\varepsilon)}{\pi} k \frac{F}{x^2} \quad (1)$$

where ε is the porosity of the powder bed, k is the coordination number and x is the particle size. On the basis of the relationship between porosity and coordination number, eqn (1) can be transformed into

$$\sigma = \frac{(1-\varepsilon)}{\varepsilon} \frac{F}{x^2} \quad (2)$$

Herein, we used the conventional relationship between porosity and coordination number:[32]

$$k\varepsilon = \pi \quad (3)$$

Therefore, the adhesion force can be estimated from strength measurement data in conjunction with particle size and porosity, which are basic powder properties. Note that chemical characteristics are not included in the Rumpf theory. Chemical characteristics directly influence adhesion force. For example, the van der Waals force, F_v, between two uniform particles is described by the following equation:

$$F_v = \frac{Ax}{24H^2} \quad (4)$$

where H is the surface distance and A is the Hamaker constant. Given the adhesion mechanism of ash particles, the liquid bridge force is the dominant adhesion force. The liquid bridge force, F_l, is described by the following equation:

$$F_l = \pi x \gamma \cos\theta \quad (5)$$

where γ is the surface tension and θ is the contact angle. Parameters A, γ and θ are affected by chemical characteristics. Notably, the adhesion force can be estimated from strength using the Rumpf equation, and the estimated force is affected by several parameters related to ash chemistry.

Note that the physical characteristics of ash, the porosity of the powder bed and the particle size also affect the measured strength.[6] When investigating the relationship between adhesion behaviour and ash chemistry using strength datasets, it is necessary to pay attention to the effects of physical characteristics.

To investigate ash adhesion, it is necessary to measure the strength of an ash powder bed at high temperatures simulating the conditions inside a thermochemical conversion plant. Nevertheless, most of the devices for measuring the strength of a powder bed are designed for measurement at room temperature.[27b,c,33] We have developed equipment to measure the tensile strength of a powder bed at high temperatures. A schematic of the developed device is shown in Fig. 6.[34] The horizontal split cells made of quartz consist of a movable part and a fixed part. Particulate samples are introduced into the cylindrical parts, and a powder bed is formed by packing. Tensile tests of the powder bed are performed by pulling the movable part. Because the cells are suspended in the furnace, tensile tests can be performed at high temperatures and the effect of friction is negligible. The tensile strength of the powder bed can be determined by tensile tests with good repeatability (standard deviation less than 25%); the results are shown in the following sections. In ash adhesion research, it is important to measure not only the adhesive force between particles but also that between particles and walls. An effective method for measuring the force between particles and walls is to contact a powder bed of ash with a metal surface simulating a heat exchanger and then conduct tensile or shear tests between the powder bed and the metal. Devices for measuring tensile and shear strength between ash deposits and metal surfaces have been designed and developed by Laxminarayan *et al.*, who used them to effectively understand the adhesion of biomass ash.[35] We also developed a shear-strength measurement device (Fig. 7) by modifying a tensile-strength measurement device (Fig. 6) to measure the shear strength between the powder bed and metal at high temperatures.[36]

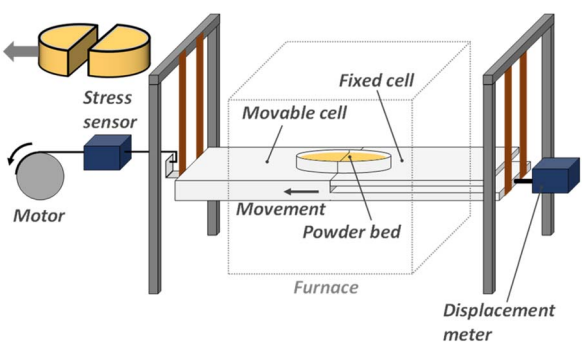

Fig. 6 Schematic view of the tensile strength tester.[34]

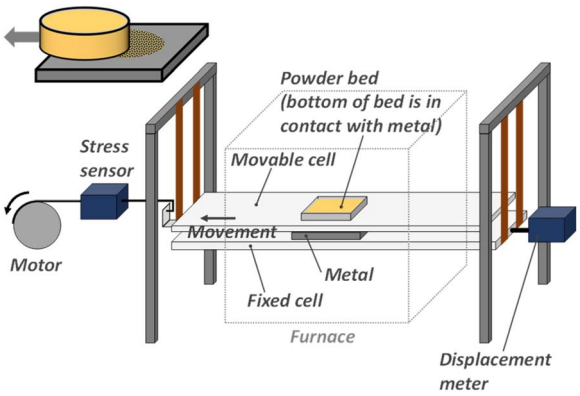

Fig. 7 Schematic view of the shear strength tester.[36a]

Understanding adhesion behaviour in the commercial plants: use of 'real' ash

Ash adhesion has been studied using 'real' ash produced from commercial industrial plants, such as coal-fired power generation and biomass combustion/gasification plants. Originally, investigations of ash adhesion at high temperatures were conducted using coal combustion ash. Recently, as more attention has been focused on the use of biomass and waste as fuels, interest has expanded to include ash derived from these sources. Nonetheless, the results and research methods used with coal ash may be directly applicable to investigations of biomass and waste ashes.

Statistical analysis is important in investigations using real ashes because of the complexity and variety of their chemical characteristics. To investigate the relationships between chemical characteristics and ash adhesion, it is useful to use numerous types of ashes with different chemical characteristics. Using a phase diagram is a valuable way to summarise many datasets and to understand the relationships between chemical characteristics and ash adhesion. As a typical example, a ternary graph can be created by classifying the elements in the ash into three groups.[37] The chemical components of the various ashes are plotted in the ternary graph. In addition, introducing the ash fusion temperatures of each ash into the graph enables the observation of trends in the relationship between the chemical characteristics and fusion temperature of the ash. This method was originally applied to understand the melting behaviour of coal ash and has recently been used to investigate biomass ash.[37] Vassilev and coworkers investigated the correlations and associations among chemical characteristics using 86 samples of biomass ashes.[38] On the basis of the strong and significant correlations between chemical characteristics, the elements in the ashes were grouped into three sets: Si–Al–Fe–Na–Ti, Ca–Mg–Mn and K–P–S–Cl.[39] The authors created a ternary graph using the three groups and plotted the chemical compositions of various ashes on the graph (Fig. 8).[37b,38b] The compositional regions of the coal ash were localised, whereas the compositional regions of the biomass ash were broad, suggesting a greater variety of chemical properties for the biomass ashes. In the next step, the

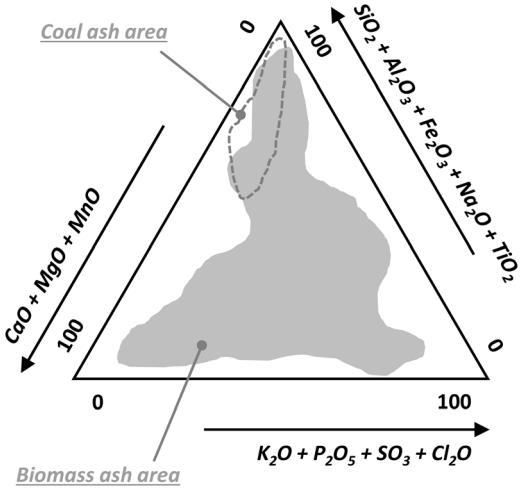

Fig. 8 Area for chemical components of coal and biomass ash in the chemical classification system.[37b,38b]

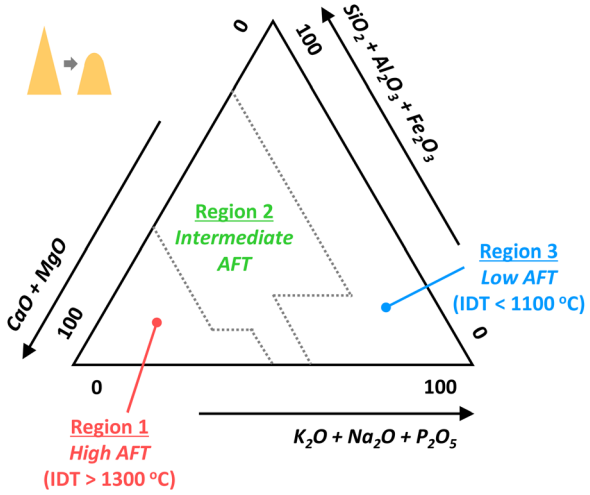

Fig. 10 Grouping for chemical compounds of biomass ash based on their ash fusion temperature (AFT). The initial deformation temperature (IDT) was used.[40]

authors plotted the ash fusion temperatures on the ternary graph (Fig. 9), revealing several trends.[37b] The initial deformation temperature (IDT), one definition for the ash fusion temperature, is plotted in the graph in Fig. 9. A higher content of Si, Al, Ca and Mg tended to increase the ash fusion temperature, which can be predicted to result in lower adhesion at high temperatures. By contrast, lower contents of these elements and higher contents of K and P resulted in a low ash fusion temperature. Thus, high adhesion can be predicted at high temperatures.

Lachman *et al.* created a ternary graph based on the works of Vassilev and introduced it as a relatively reliable method for predicting adhesion (Fig. 10).[40] They used the initial deformation temperature (IDT). Note that the three sets of element groups differed slightly from that reported by Vassilev *et al.* (Fig. 8 and 9).[37b,38b] Lachman *et al.* chose eight abundant elements (oxides). K and Na were grouped with P because these elements were found to be the abundant elements in the samples with lower ash fusion temperatures. The graph was divided into three regions based on the ash fusion temperature. Region 1 contained higher amounts of Ca and Mg, corresponding to higher ash fusion temperatures, and consisted mainly of woody biomass. By contrast, region 3, with high contents of K, Na and P, showed a lower ash fusion temperature and consisted of straw, grasses, flowers and chicken and cattle manures. The authors recommended that, when the biomass categorised in region 3 is used as fuels, additives should be used to suppress adhesion; they also recommended co-firing with less problematic fuels categorised in region 1.

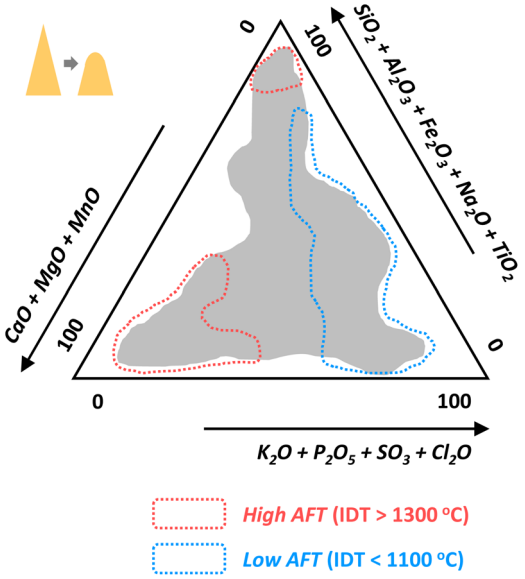

Fig. 9 Area of low and high ash fusion temperatures (AFTs) for biomass ash in the chemical classification system. The initial deformation temperature (IDT) was used.[37b]

The AFT is often used as an index to evaluate ash adhesion. Notably, the measured temperatures are generally higher than 1000 °C but ash adhesion can be observed at temperatures lower than 1000 °C in commercial plants. The AFTs are determined by the deformation of ash pellets at elevated temperatures, which requires the formation of a sufficient amount of molten phase. To evaluate ash adhesion at plant operating temperatures, which are lower than AFTs for most ashes, we measured the tensile strength of an ash powder bed at temperatures less than 1000 °C using the homemade device described above.[34] The tensile strengths of coal and sewage–sludge ashes were measured and found to increase in strength at 600–900 °C (Fig. 11).[16a,d] These valuable results quantitatively demonstrated the increase in ash adhesion at plant operating temperatures. We used our homemade CC-SEM in combination with a heat-treatment chamber to observe microscopic morphological changes of coal ash before and after heat treatment and observed partial melting of the ash particle surface after the heat treatment at 900 °C, which is the temperature at which the tensile strength increased (Fig. 12).[16a,e] Notably,

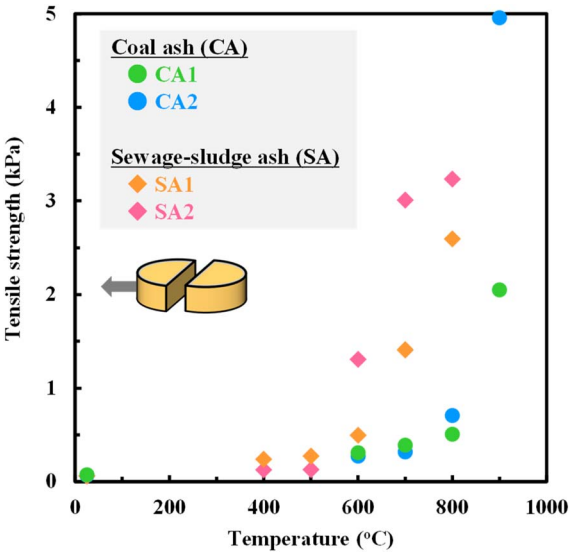

Fig. 11 Tensile strength of powder bed with coal and sewage–sludge ashes, plotted as a function of temperature.[16a,d]

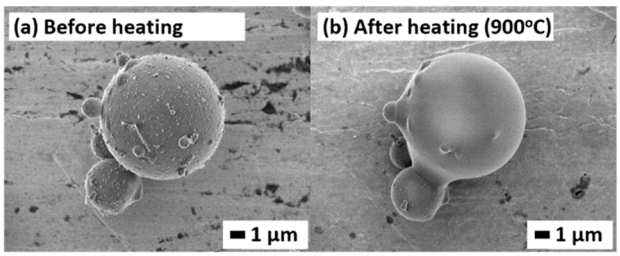

Fig. 12 FE-SEM images of coal ash particles (a) before and (b) after heating at 900 °C.[16a]

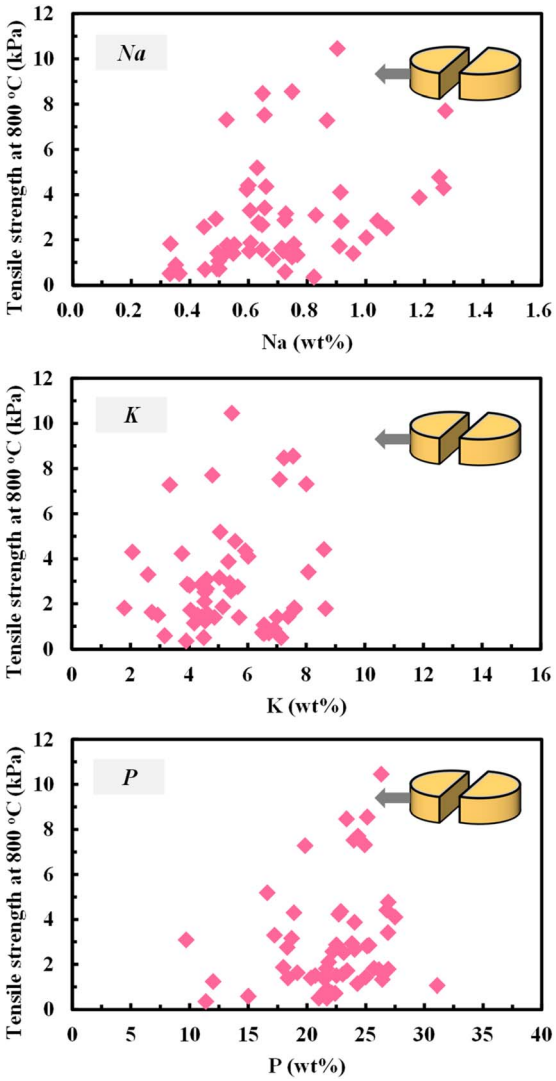

Fig. 13 Tensile strength of powder bed with sewage–sludge ashes as a function of their chemical composition.[41]

partial melting was observed, with no apparent deformation of the powder bed observed under the same conditions. From the calculation of the liquid bridge force, the observed small amount of molten phase (*i.e.*, the ratio of volume to single-particle volume, on the order of parts per billion) was sufficient to increase the observed tensile strength at 900 °C.[16a] In addition, we observed a difference in the temperature at which the tensile strength started to increase between coal and sewage–sludge ashes. The tensile strength of the sewage–sludge ashes containing P started to increase at 600 °C, which was lower than the corresponding temperature for coal ash without P. The results suggested that the effects of Na, K and P on adhesion were different. This point was investigated using synthetic ashes, as described below. To investigate relationships between ash characteristics and tensile strength, we measured the tensile strength of 56 samples of sewage–sludge ashes.[41] Although various tensile strengths were measured, significant relationships between the Na, K and P concentrations and tensile strength were not observed (Fig. 13). In this case, we reported a stronger correlation between physical characteristics (particle size and porosity of powder bed) and tensile strength but did not exclude the influence of chemical composition. These results suggest that examining the relationship between ash chemistry and adhesion in real ash is difficult and that factors other than chemical characteristics need to be considered.[16a,b]

Our ability to discuss the effects of chemical characteristics on ash adhesion at high temperatures on the basis of the results obtained using real ash is limited. Although the use of ternary graphs can aid in evaluating the effects of chemical characteristics on ash adhesion and in predicting adhesion, understanding the difference in the effects among elements grouped in the same sets is difficult. For example, in the analysis using ternary graphs, K and P (and in some cases Na) were grouped together in the same sets. However, our results using a tensile strength tester indicated that the role of P in particle adhesion was different from that of Na and K and that the roles of Na and K would be different.[42] In addition, although Si and Al were grouped in the same set in the above ternary graphs, their roles in ash adhesion were suggested to be different.[43] These points

are essential for understanding and evaluating ash adhesion; however, further discussion based on the results using real ash, which has a complicated and uncontrollable chemical composition, is unlimited. Although the analysis of real ash is important for understanding real behaviour that occurs in commercial plants, the use of materials with simple and controllable chemical composition is useful for mechanistic understanding of the detailed effects of chemical composition on particle adhesion.

Mechanistic understanding of ash adhesion: use of 'synthetic' ash

To understand the effect of chemical characteristics on ash adhesion at high temperatures, the use of model compounds is effective.[44] Specifically, compounds that have simple chemical components and that partially simulate the properties of real ash are prepared from pure materials. In this review, model compounds of ash are referred to as 'synthetic' ashes. The adhesion properties of synthetic ashes will be evaluated using methods similar to real ash analysis methods such as measurements of the ash melting temperature and tensile strength. In addition, the chemical composition of the synthetic ashes is controllable, and it may be possible to determine detailed chemical properties, such as the concentration of target elements and the presence/absence of coexisting elements, and to correlate chemical properties with adhesion. Because of these advantages and potential applications, researchers have used synthetic ashes in recent years to investigate the mechanisms of ash adhesion.

There are several types of synthetic ashes with different design concepts, which can be categorised into two types based on their similarity to real ashes (Fig. 14). One of the concepts is to simplify real ashes and use synthetic ashes that simulate real ashes. Synthetic ashes are prepared to partially simulate the chemical compositions of real ashes but are composed of selected elements (species). Usually, more than four components are selected from the real ash. Those pure materials are used as precursors, and the synthetic ashes are obtained by heating the mixtures of precursors. Synthetic ashes prepared according to this concept have chemical components similar to those of real ashes and are useful for understanding the behaviour observed in real ashes. The other type of synthetic ashes is simple systems consisting of only 2–3 components that are the focus of attention; these ashes are used to understand the effects of specific components (elements) or specific interactions. Synthetic ashes are prepared with various concentrations of target elements (species) and base components (stable components). They are useful for understanding the effect of a target element's concentration on particle adhesion. In addition, to understand the interactions between specific components, only two components are mixed and heated and the resultant synthetic ash is characterised. Thus, the synthetic ash is prepared from the target components only and consists of two or three components. It is not a copy of the actual ash; it is a simple mixture that offers a mechanistic understanding of the behaviour that can occur in real ash.

Synthetic ashes with simple and controlled chemical characteristics can contribute to the mechanistic understanding of ash behaviour related to ash chemistry. On the other hand, real ash is more useful than synthetic ash in obtaining an overview of the real behaviour occurring in commercial plants and in presenting operational issues. It should be noted that synthetic ash cannot completely simulate real behaviour and is only a useful tool to provide a mechanistic explanation of real behaviour. It is important to select and use either synthetic ash or real ash appropriately according to objectives.

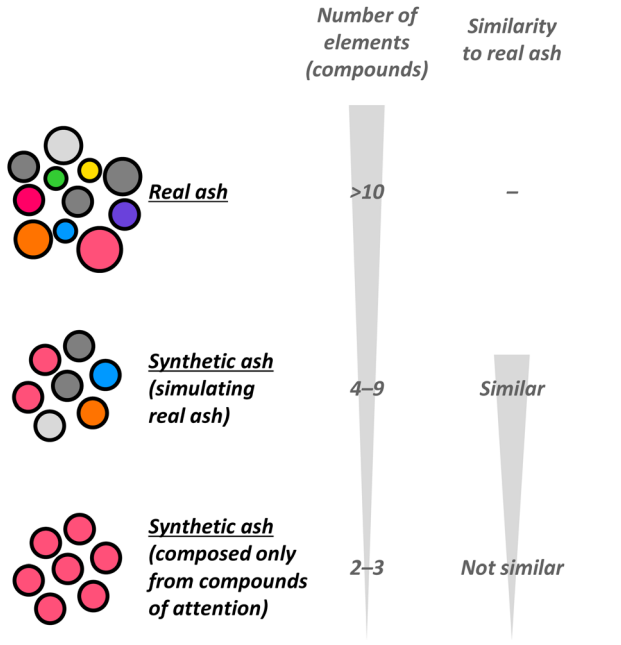

Fig. 14 Categorisation of synthetic ash.

Synthetic ash simulating a component of real ash

The synthetic ashes presented in this section are copies of real ashes, but some trace components are excluded.[45] The mixing ratios of certain components are sometimes varied to elucidate the effects of concentration changes.

Studies using synthetic ashes simulating coal ashes are presented and summarised in Table 4. Hu and coworkers focused on the SiO_2–Al_2O_3–CaO–Fe_2O_3–K_2O system in coal ashes and prepared synthetic ashes with these five components mixed in various ratios.[46] The AFTs of the synthetic ashes were measured to investigate the effects of the mixing ratios of these components. The AFTs decreased with increasing Fe_2O_3 content. X-ray photoelectron spectroscopy (XPS) studies suggested that increasing the Fe_2O_3 content promoted a change of the Fe valence from Fe^{3+} to Fe^{2+}. The presence of Fe^{2+} (*i.e.*, as FeO) would lead to the formation of a eutectic mixture. The temperatures decreased rapidly with increasing SiO_2/Al_2O_3 ratio until the ratio reached ~1.5. At higher SiO_2/Al_2O_3 ratios, the AFT slightly decreased or remained stable. The observed decrease in the AFT was due to the mineral compositions. The dominant mineral species were high-melting corundum at low SiO_2/Al_2O_3

Table 4 Summary of findings obtained from synthetic ash simulating coal ash[a,b]

Components	Method used to evaluate adhesion	Parameter related to adhesion	Ref.
SiO_2–Al_2O_3–CaO–Fe_2O_3–K_2O	AFT	Fe_2O_3 content Fe_2O_3 increases → AFT decreases SiO_2/Al_2O_3 ratio SiO_2/Al_2O_3 increases (<1.5) → AFTs decrease SiO_2/Al_2O_3 increases (1.5<) → AFTs slightly increase (or remain stable) CaO CaO increases (<30%) → AFT decreases CaO increases (30%<) → AFT increases	46
SiO_2–Al_2O_3–CaO–Fe_2O_3	AFT	SiO_2/Al_2O_3 ratio SiO_2/Al_2O_3 increases (<2.5) → AFTs rapidly decrease	47*a*
	TMA	SiO_2/Al_2O_3 increases (2.5<) → AFTs slightly increase (or remain stable)	
SiO_2–Al_2O_3–CaO–Fe_2O_3	AFT	CaO/Fe_2O_3 ratio CaO/Fe_2O_3 increases → AFTs increase	47*b*, and 47*c*
	TMA	Fe valence Addition of Fe^{2+} → AFT decreases	

[a] AFT = Ash fusion temperature. [b] TMA = Thermomechanical analysis.

ratios and low-melting anorthite and gehlenite at high SiO_2/Al_2O_3 ratios. In addition, the AFT decreased with increasing CaO content, reaching a minimum when the CaO content approached 30% and then increasing when the CaO content was increased further. The observed CaO effect was also explained by mineral species. By contrast, no significant effect of the K_2O content on the AFT was observed, which was attributed to the K_2O content not affecting the mineral species. These results suggested that changing the mineral species associated with changes in elemental compositions strongly affected the ash fusion characteristics, specifically ash adhesion.

Bai and coworkers also prepared synthetic ashes that simulated coal ashes and studied the effects of certain characteristics.[47] They prepared a synthetic ash consisting of the SiO_2–Al_2O_3–CaO–Fe_2O_3 system and investigated the effects of the SiO_2/Al_2O_3 and CaO/Fe_2O_3 ratios using the AFT as an index of particle adhesion.[47a,b] They found that the AFT rapidly decreased with increasing SiO_2/Al_2O_3 ratio until the ratio reached ~2.5. The trend was similar to that observed in the previously discussed study of the SiO_2–Al_2O_3–CaO–Fe_2O_3–K_2O system.[46] They also showed that the effect of the SiO_2/Al_2O_3 ratio depended on the CaO content. When synthetic ashes with low CaO contents were used, the AFT decreased with increasing SiO_2/Al_2O_3 ratio, reaching a minimum temperature when the SiO_2/Al_2O_3 ratio approached 2.5 and then slightly increasing as it was increased further. For synthetic ashes with a high CaO content, even though a similar trend was observed in the region where the SiO_2/Al_2O_3 ratio was less than 2.5, the AFT remained stable when the SiO_2/Al_2O_3 ratio was greater than 2.5. These results indicated that explaining the AFT—specifically, ash adhesion—with a single index is difficult. The AFT increased with increasing CaO/Fe_2O_3 ratio. The effect of the CaO/Fe_2O_3 ratio was explained on the basis of the Fe_2O_3 content and the Fe valence, similar to the explanation in the previously discussed study.[46] A decrease in the CaO/Fe_2O_3 ratio—specifically, an increase in the Fe_2O_3 fraction and a decrease in the CaO fraction—changed the Fe valence from Fe^{3+} to Fe^{2+}. The effect of the Fe valence was also investigated in a study that used synthetic ash prepared from different Fe precursors, and the addition of Fe^{2+} to synthetic ash with a low CaO content was demonstrated to promote the eutectic reaction of the Si–Fe–O system and to accelerate liquid formation.[47c]

The behaviour of synthetic ashes designed to simulate real coal ashes was compared with that of real ashes. Hu and coworkers reported the chemical compositions of seventeen types of coal ash, providing a design basis for synthetic ash and a method for controlling the AFT.[46] The AFTs of real coal ashes decreased with increasing SiO_2/Al_2O_3 ratio and increasing Fe_2O_3 content, and the trends were similar to those observed for synthetic ashes. Song and coworkers studied composition-controlled real coal ashes.[48] Specifically, they added SiO_2, Al_2O_3, CaO, Fe_2O_3 and MgO to real coal ashes with various mixing ratios to investigate the effect of chemical characteristics on the AFT. The effect of the CaO and Fe_2O_3 contents on the AFTs of component-controlled real coal ash showed a trend similar as their effect on the AFTs of the synthetic ashes. By contrast, the effect of the SiO_2/Al_2O_3 ratio on the AFTs of the real ash system did not agree with that of the synthetic ashes. The AFTs of the real ash system increased with increasing SiO_2/Al_2O_3 ratio, whereas the opposite trend was observed for the AFTs of the synthetic ashes. The observed behaviour in real ashes was explained by mineral species. The main mineral species was low-melting anorthite for low SiO_2/Al_2O_3 ratios and high-melting mullite and corundum for high SiO_2/Al_2O_3 ratios. The observed relationships between the types of mineral species and the SiO_2/Al_2O_3 ratio were opposite from those of synthetic ash.[46] As a typical example of these findings, the effect of the SiO_2/Al_2O_3 ratio on ash adhesion has been investigated using not only synthetic ashes but also coal ashes, and the conclusions are not consistent (Table 5). Basically, these inconsistent conclusions are attributable to mineral compositions. In addition, numerous parameters such as mineral formation reactions and coexisting elements can lead to different conclusions.

Table 5 Comparison of real coal ash and synthetic ash regarding the effect of the SiO_2/Al_2O_3 ratio on adhesion[a,b]

Real/synthetic	Method used to evaluate adhesion	Relationship between SiO_2/Al_2O_3 ratio and adhesion property	Ref.
Real (blending)	TMA calculation	SiO_2/Al_2O_3 increases →Suppresses fusion	43*a*
Real	AFT	SiO_2/Al_2O_3 increases →AFT decreases	46
Real + pure	AFT	SiO_2/Al_2O_3 increases →AFT increases	48
Synthetic (SiO_2–Al_2O_3–CaO–Fe_2O_3–K_2O)	AFT	SiO_2/Al_2O_3 increases (<1.5) → AFTs decrease SiO_2/Al_2O_3 increases (1.5<) → AFTs slightly increase (or remain stable)	46
SiO_2–Al_2O_3–CaO–Fe_2O_3	AFT TMA	SiO_2/Al_2O_3 increases (<2.5) → AFTs rapidly decrease SiO_2/Al_2O_3 increases (2.5<) → AFTs slightly increase (or remain stable)	47

[a] AFT = Ash fusion temperature. [b] TMA = Thermomechanical analysis.

Bryant and coworkers investigated using blending coals with different chemical compositions to control the SiO_2/Al_2O_3 ratio.[43a] The ash fusion characteristics were determined using thermomechanical analysis (TMA) and thermodynamic calculations. Increasing the SiO_2/Al_2O_3 ratio suppressed ash fusion. A conclusion concerning the effect of the SiO_2/Al_2O_3 ratio on ash adhesion was difficult to reach because the effect of the SiO_2/Al_2O_3 ratio depends not only on the mineral species but also on the reactions for mineral formation. The reaction is expected to be affected by the raw materials (*i.e.*, the origin of Si and Al), the temperature at which the ash forms (*i.e.*, the operating temperature of the plant), and the reaction atmosphere (*i.e.*, combustion or gasification). In addition, the effect of the SiO_2/Al_2O_3 ratio may depend on coexisting elements. In particular, the presence of Na, K and P, which form eutectic mixtures with SiO_2, is expected to affect the adhesion behaviour. Given the various factors related to ash formation, care is required to investigate the effect of the SiO_2/Al_2O_3 ratio. Bai and coworkers reported a comparison study between real coal ash and synthetic ash.[49] The synthetic ash used in their study was composed of the SiO_2–Al_2O_3–Fe_2O_3–CaO–MgO–$CaSO_4$–TiO_2–K_2CO_3–Na_2CO_3 system. The difference in mineral compositions between real and synthetic ash resulted in differences in the ash fusion characteristics. To match mineral compositions between real ash and synthetic ash, synthetic ash should be prepared under appropriate conditions using appropriate precursors.

Studies using synthetic ashes simulating biomass and waste ashes as energy feedstocks have recently been reported. To understand the adhesion of biomass and waste ashes, findings from coal ash studies may be useful; however, it is necessary to study the effects of unique elements contained in biomass and waste ashes, such as Cl and P.[12a,b,14]

Liu, Yu and coworkers studied the effect of P using synthetic ash consisting of SiO_2, Al_2O_3, CaO, Fe_2O_3, Na_2O and P_2O_5, with various Al_2O_3/CaO ratios.[50] They found that the effect of P on the AFT depended on the Al_2O_3/CaO ratio and proposed a mechanism based on mineral species. For low Al_2O_3/CaO ratios, the ash melting temperature tended to decrease and then increase with increasing P fraction. In this case, a small amount of P promoted the formation of $CaSiO_3$ (wollastonite)–$Ca_3(PO_4)_2$ (apatite) eutectic mixtures, leading to a decrease in the AFT. The addition of large amounts of P caused apatite-dominant ash, resulting in an increase in the AFT as a result of the high melting point of apatite. For high Al_2O_3/CaO ratios, the AFT decreased with increasing P content because of the formation of $AlPO_4$ (berlinite)–SiO_2 eutectic mixtures. Liu, Yu and coworkers also concluded that the addition of P prevented the formation of aluminosilicate and corundum, which have high melting points, suggesting that P exhibited high reactivity with Al.

In the thermochemical conversion of biomass and waste, the corrosion of heat exchangers due to ash adhesion must be considered. Lindberg, Niemi, Balint and coworkers used synthetic ash in an investigation of the mechanism of biomass ash deposition on a superheater and the corresponding corrosion.[44,51] The synthetic ash was prepared by selecting 2–4 compounds from among NaCl, NaBr, Na_2SO_4, KCl, KBr and K_2SO_4. Simulated superheater deposits were prepared using the synthetic ash. This study using synthetic ash with simple chemical characteristics offered convincing information about the effect of temperature gradients in the deposits, the morphology of the deposits and their migration behaviour.

The synthetic ashes introduced in this section were designed and prepared on the basis of the chemical compositions of real ashes and the partially simulated behaviour of real ashes. The simplified chemical composition of the synthetic ashes was beneficial for understanding the detailed mechanism of ash adhesion. The studies using synthetic ashes provided important insights, such as the necessity of considering the effects of various factors to understand the adhesion behaviour of real ash, which has a complex chemical composition. Synthetic ash is a powerful tool for evaluating complex effects such as those of the SiO_2/Al_2O_3 ratio because it can be prepared by experimentally controlling parameters that affect characteristics. However, preparing synthetic ash that simulates real ash requires that the composition be designed not only to match the elemental composition but also contain similar mineral species.[49] In addition, although synthetic ash simulating real ash was used, the behaviours observed with real ash were difficult to explain, reflecting the complexity of ash chemistry.[49] These difficulties highlight the importance of using an approach in which the interactions between elements are studied individually in simpler models, such as systems composed of two or three

elements (components), followed by an analysis of the behaviour based on the fundamental findings.

Synthetic ash to elucidate the effects of specific elements, components and interactions: using a very simple system

Investigating the effect of a single factor—the concentration of target elements or specific interactions between components—on particle adhesion is also important and can provide basic information for elucidating the complex adhesion behaviour of real ash.[52] Specifically, relationships between chemical characteristics (*e.g.*, the concentration of target elements, the types of mineral species and a specific interaction between components) and particle adhesion are investigated. For this objective, synthetic ash with simple and well-designed chemical characteristics is suitable. In this case, a synthetic ash that simulates real ash is not necessary; the important design concept is that the synthetic ash should consist of only specific elements (components). Specifically, the synthetic ash should be prepared from 2–3 precursors and its chemical characteristics should be easy to determine (Fig. 15). In addition, synthetic ashes with very simple system are useful for studying the impact of trace compounds in the real ash. The impacts of such trace compounds are expected to be difficult to detect in real ash and simulated synthetic ash because they are hidden by the effects of other compounds. Simple synthetic ashes that can focus on specific elements are effective.

Laxminarayan *et al.* conducted studies using synthetic ashes containing Si, S, Cl, K and Ca, simulating biomass ash (Fig. 16 and Table 6).[35] The noteworthy aspect of their studies was their development of a method for evaluating the adhesion of synthetic ashes. They developed devices to carry out high-temperature measurements of tensile and shear strengths between ash deposits and metal surfaces, simulating ash deposited onto the surface of a superheater. Synthetic ash consisting of KCl and K_2SO_4 was used as a standard, and it exhibited high strength. To investigate the effects of chemical

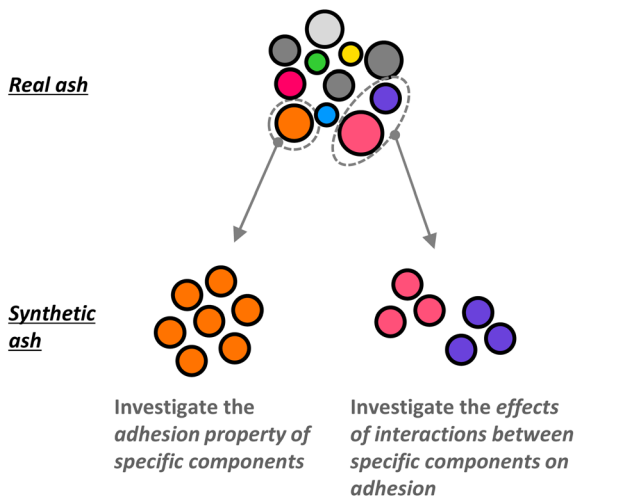

Fig. 15 Schematic of the design concept and objectives for synthetic ash using a very simple system.

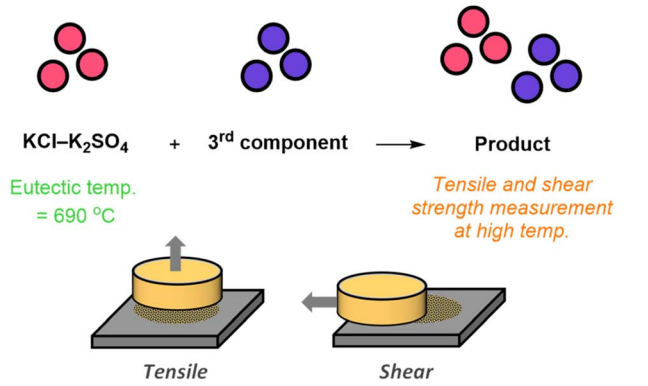

Fig. 16 Investigation biomass ash chemistry using synthetic ash with tensile and shear strength measurements.[35]

composition, one component was selected from among CaO, $CaSO_4$, Fe_2O_3, SiO_2, $K_2Si_4O_9$, K_2CO_3 and KOH and added to standard synthetic ash. That is, the effects of the interaction among KCl, K_2SO_4 and the selected third component on adhesion were investigated; the results are summarised in Table 6. Basically, strength increased in systems where the eutectic temperature decreased with the addition of a third component. The researchers observed this phenomenon by adding $CaSO_4$, Fe_2O_3, K_2CO_3 and KOH. By contrast, the addition of CaO reduced the strength because CaO did not form a eutectic mixture with KCl and K_2SO_4 and because the presence of CaO resulted in a lower fraction of the slag phase. The addition of $K_2Si_4O_9$ further increased the tensile and shear strengths, suggesting that the presence of silicate increased ash adhesion. These results also indicate that the mineral species strongly affected ash adhesion and corrosion.

Kim, Namkung and coworkers investigated the effect of P on ash adhesion in the thermochemical conversion of sewage sludge (Fig. 17 and Table 7).[53] They investigated P-related ash chemistry using synthetic ashes prepared from P_2O_5 (precursor

Table 6 Effects of third component addition to KCl–K_2SO_4 system on adhesion strength[35a]

Entry	Third component	Eutectic temperature (°C)	Change in strength (compared to KCl–K_2SO_4) Tensile	Shear
1	CaO	690	↓	↓
2	$CaSO_4$	644	↑	↑
3	Fe_2O_3	577	—	↑
4	SiO_2	690	—	→
5	$K_2Si_4O_9$	650	↑	↑
6	K_2CO_3	580	—	↑
7	KOH	288	—	↑

[a] ↑ Strength increased compared with that of KCl–K_2SO_4. → Strength did not change compared with that of KCl–K_2SO_4. ↓ Strength decreased compared with that of KCl–K_2SO_4. — Strength was not measured.

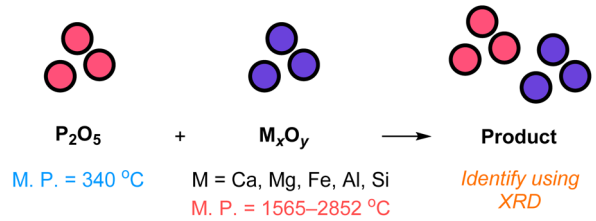

Fig. 17 Investigation of P-related ash chemistry using synthetic ash.[53]

Table 7 Summary of products formed by reaction of P_2O_5 and metal oxides (M_xO_y)[53a]

	Reactant		Product	
Entry	M_xO_y	M. P. (°C)	Product[b]	M. P. (°C)
1	CaO	2572	$Ca_3(PO_4)_2$	1670
			$Ca_2P_2O_7$	1353
2	MgO	2852	$Mg_3(PO_4)_2$	1184
			$Mg_2P_2O_7$	1383
3	Fe_2O_3	1565	$FePO_4$	1240
4	Al_2O_3	2072	$AlPO_4$	1460
			$Al(PO_3)_3$	1527
5	SiO_2	1710	Not detected	—

[a] M. P. = melting point. [b] Detected by XRD.

of P) and a target compound selected from among CaO, MgO, Fe_2O_3, Al_2O_3 and SiO_2. They used synthetic ash as a powerful tool to analyse P-related interactions. The P_2O_5-containing mixture used as a synthetic ash precursor was treated at 800–1000 °C, which is the temperature range used in sewage treatment plants. Morphological observations and XRD studies of the resultant mixtures were performed to evaluate the interactions. Compared with experiments using single minerals without P, experiments using the mixture of minerals with P showed substantial expansion and agglomeration, suggesting that the P and minerals interacted. The species formed by the interactions were characterised by XRD analysis and are listed in Table 7, along with their melting points. The products containing P had lower melting points than the single minerals, suggesting that interactions with P led to a decrease in the melting point and to ash adhesion. For the mixture of P and SiO_2, although morphological changes were observed after heat treatment, no new compounds were detected. Even though the details were not provided, part of the P likely evaporated because the heat-treatment temperature was higher than the boiling point of P_2O_5, and new compounds not detected were formed because of the interaction.

We studied the effect of chemical characteristics (types and concentrations of target elements) on particle adhesion. Our synthetic ashes were designed to consist of only two parts: the target element and the base materials (Fig. 18(a)). The target elements have the potential to induce the formation of components with low melting points, resulting in high particle adhesion. We selected Na, K and P as the target elements. The base materials were stable and did not show high adhesiveness.

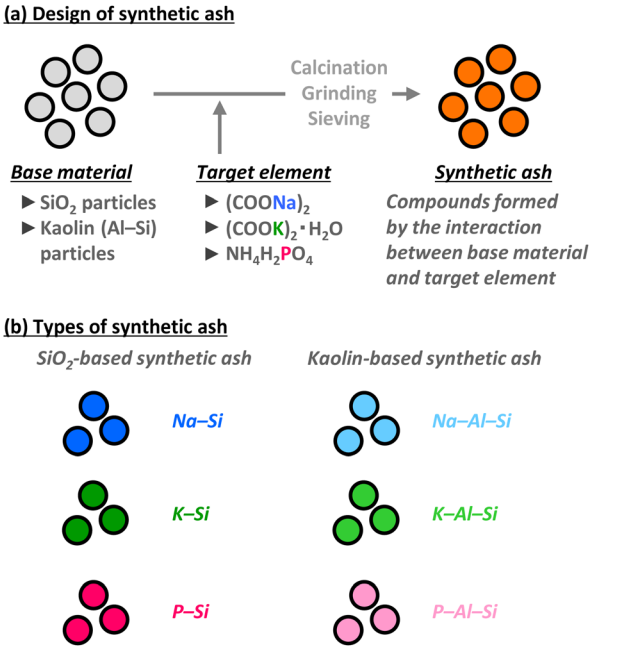

Fig. 18 Design concept of our synthetic ash to study the role of specific elements.

In addition, we selected base materials that are contained in the ash and/or bed material of the fluidised bed system and that have the potential to interact with the target elements. On the basis of this consideration, we selected SiO_2 and kaolin (a mixture of SiO_2 and $Al_2Si_4O_{10}(OH)_2$) as the base materials. This design enabled us to evaluate the adhesion characteristics of the compounds formed by the interaction between target elements and base materials. We prepared six types of synthetic ashes (Fig. 18(b)), three types of SiO_2-based ashes (Na–Si, K–Si and P–Si) and three types of kaolin-based ashes (Na–Al–Si, K–Al–Si and P–Al–Si).[42] The particle adhesion of the synthetic ashes was quantified using our homemade device for measuring the tensile strength of a powder bed, as described in the preceding section.

SiO_2-based synthetic ashes were prepared with various concentrations of target elements, and the relationships between tensile strength at 900 °C and the concentration were investigated (Fig. 19). A similar trend was observed in Na–Si and K–Si synthetic ashes. The tensile strength increased with the addition of a small amount of Na and K (less than 1 wt%), and the tensile strength was almost constant when the Na and K concentration was greater than 1 wt%. A different trend was observed in P-containing synthetic ash, where the tensile strength increased in proportion to the P concentration. The relationship between tensile strength and temperature was also investigated (Fig. 20), and the trend differed depending on the element. The temperature range in which the tensile strength started to increase was 500–600 °C, 600–700 °C and 800–900 °C for P–Si, K–Si and Na–Si, respectively. These temperature ranges correspond to the eutectic temperatures (slag formation temperatures determined by thermodynamic calculations) and the melting points of proposed compounds. Therefore, the

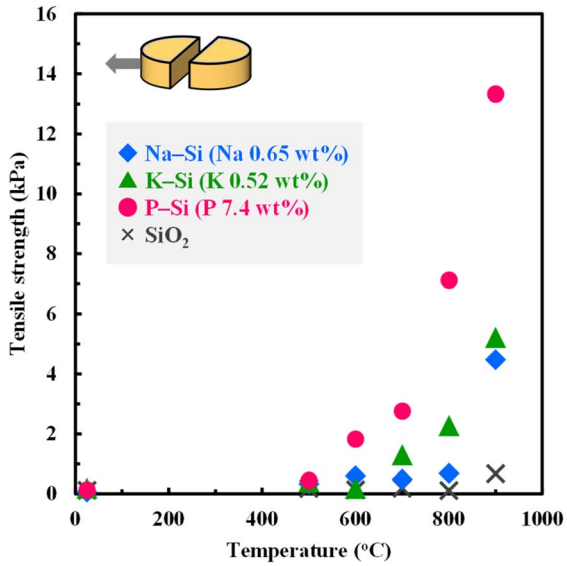

Fig. 19 Tensile strength at 900 °C of a powder bed with SiO_2-based synthetic ash (Na–Si, K–Si and P–Si), plotted as a function of the Na, K and P concentrations.[42b,d]

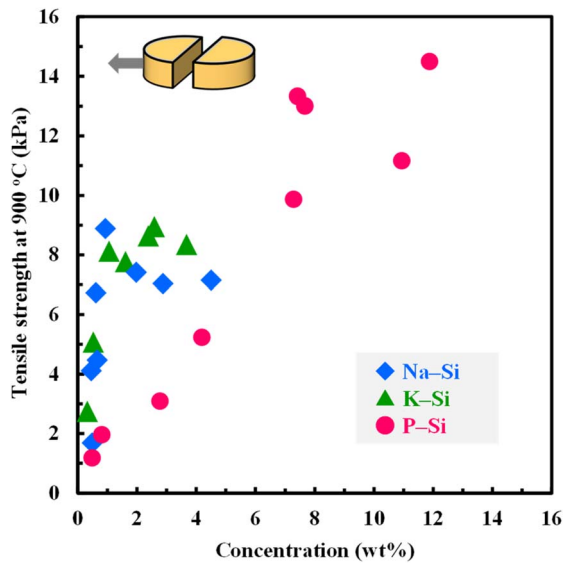

Fig. 20 Tensile strength of a powder bed with SiO_2-based synthetic ash (Na–Si, K–Si and P–Si) as a function of temperature.[42b,d]

increase in tensile strength was due to the formation of a liquid phase. The concentration dependence would be influenced by the fraction of the liquid phase; specifically, the increase in the liquid fraction resulted in an increase in tensile strength. Thermodynamic calculations suggested that, although the small amounts of Na and K induced the formation of a liquid phase, more P was required for the formation of the P-induced liquid phase (Fig. 21).

The tensile strengths of kaolin-based synthetic ashes were also measured (Fig. 22), and the observed trends differed from those of the SiO_2-based ash. For Na–Al–Si ash, the addition of

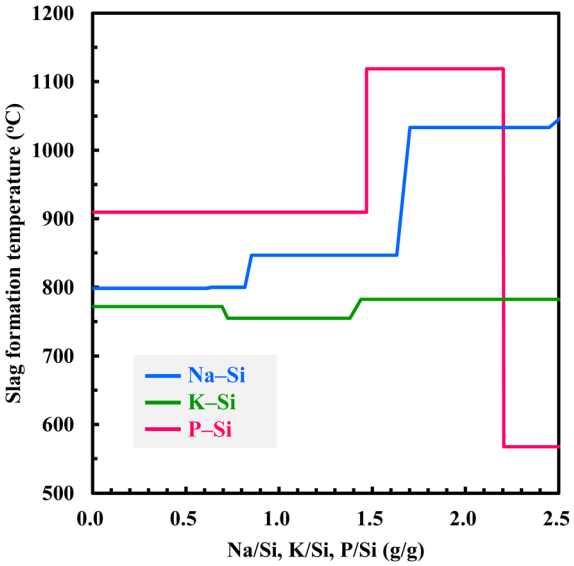

Fig. 21 Slag formation temperature of Na–Si, K–Si and P–Si systems as a function of the chemical compositions estimated using thermodynamic calculations.[42b,d]

a small amount of Na rapidly increased the tensile strength, showing a similar trend as the tensile strength of Na–Si ash. However, in the case of K–Al–Si and P–Al–Si ashes, the tensile strength slightly increased with increasing K and P concentrations until a certain concentration was reached (15 wt% for K and 25 wt% for P) and then rapidly increased as the concentration was increased further. The differences from SiO_2-based ashes are likely derived from the presence of Al in the ashes. The presence of Al increased the slag formation temperatures for the K- and P-containing systems but decreased that for the Na-containing system (Fig. 23). The calculations also suggested

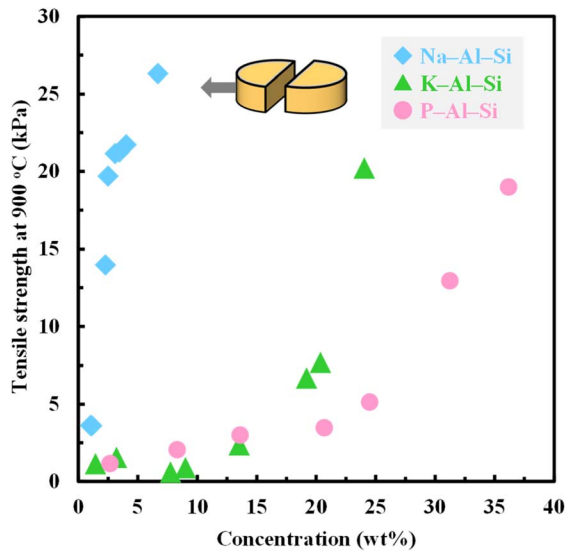

Fig. 22 Tensile strength at 900 °C of a powder bed with kaolin-based synthetic ash (Na–Al–Si, K–Al–Si and P–Al–Si) as a function of the Na, K and P concentrations.[42a,c]

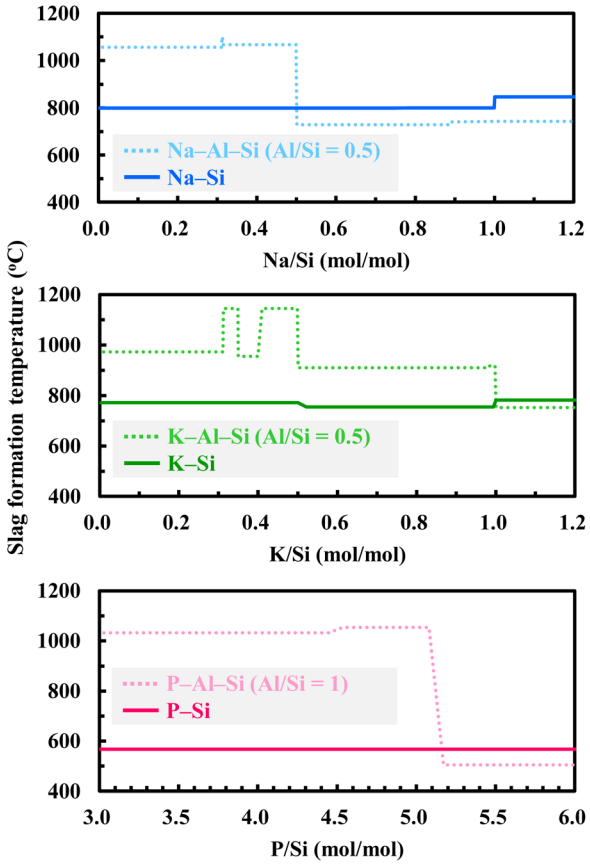

Fig. 23 Slag formation temperature of Na–Al–Si, K–Al–Si and P–Al–Si system as a function of the chemical composition estimated using thermodynamic calculations.[42]

that large amounts of K and P reduced the slag formation temperatures, indicating that adhesion increased. The tensile strength measurement results were consistent with the calculation results.

This review is focused on the ash adhesion behaviour related to the melting of ash. By contrast, sintering unrelated to melting is also a potential mechanism of ash adhesion at high temperatures. In particular, some Ca-related adhesion is due to sintering, and types of mineral species can be an important parameter.[54] Details of the sintering-derived adhesion are not discussed in this review because the mechanism differs substantially from that of melting-derived adhesion. However, we note that synthetic ash can also be used in research on Ca-related adhesion.[55]

Use of synthetic ash as an investigation method to control adhesion

The development of methods to control ash adhesion at high temperatures is important for stable and efficient plant operation. The use of additives is one approach to effectively control adhesion.[56] The addition of appropriate additives to fuels or furnaces suppresses the formation of low-melting compounds, resulting in suppression of ash adhesion. However, the use of inappropriate additives can accelerate adhesion problems because of effects such as reducing the eutectic temperature.[57] Such an undesirable phenomenon was demonstrated in the studies of Laxminarayan *et al.*, which we introduced in a previous section (Fig. 16 and Table 6).[35] The strength of synthetic ash containing $KCl–K_2SO_4$ decreased with the addition of CaO but increased with the addition of $CaSO_4$. Their results clearly demonstrated the importance of selecting appropriate compound species to effectively decrease adhesion. Using synthetic ash is a useful method for investigating appropriate additives depending on the cause of adhesion (Fig. 24). Synthetic ash, especially systems with simple chemical compositions, has clear adhesion factors, enabling the search for appropriate additives according to those factors.

We used SiO_2, Al_2O_3 and Fe_3O_4 nanoparticles as additives and investigated their effects by adding them to SiO_2-based synthetic ashes (Fig. 25).[16c] Highly reactive nanoparticles were used to elucidate the effect of ash–additive relationships on adhesion. The tensile strength of the synthetic ash with and without additives was measured at 900 °C (Fig. 25 and Table 8). The results suggest that appropriate types of additives should be selected according to the cause of adhesion. In particular, Al_2O_3 nanoparticles reduced the tensile strength of Na–Si, K–Si and P–Si synthetic ashes. By contrast, the effect of SiO_2 nanoparticles was weaker than that of Al_2O_3 nanoparticles. Thermodynamic calculations suggested that the addition of Al resulted in the formation of high-melting compounds. By contrast, the further addition of Si could promote slag formation. In fact, Al_2O_3 nanoparticles were found to decrease the melting point of real ashes in a demonstration using Na- and K-

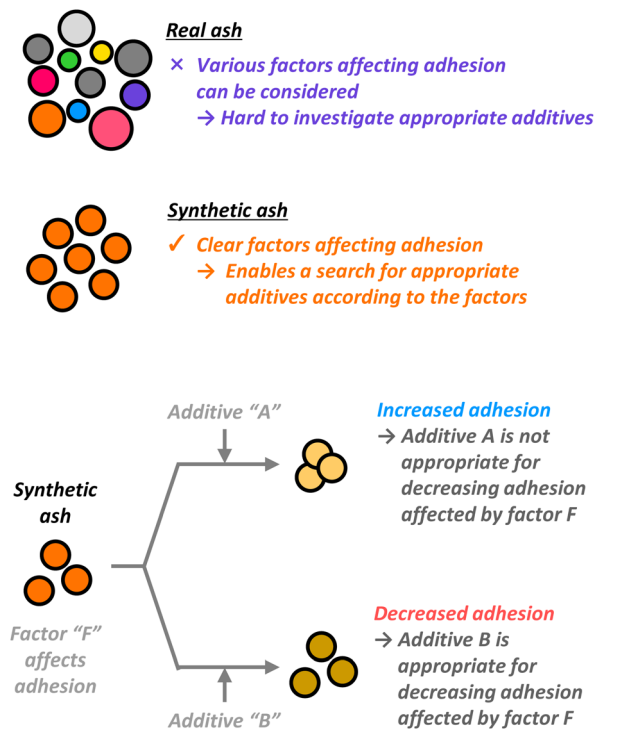

Fig. 24 Advantage of synthetic ash in investigations of appropriate additives to decrease adhesion.

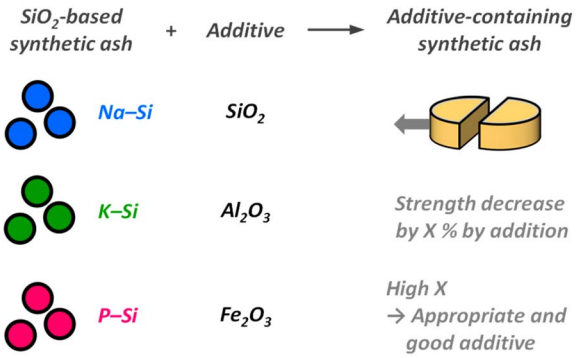

Fig. 25 Schematic of a method for studying appropriate additives using synthetic ash.

Table 8 Decrease in tensile strength at 900 °C (X) with the addition of SiO_2, Al_2O_3 and Fe_2O_3 additives to Na–Si, K–Si and P–Si synthetic ashes[16c]

	X (%)			
	Additive	SiO_2	Al_2O_3	Fe_2O_3
Synthetic ash	Na–Si	33	**83**	3
	K–Si	62	**91**	8
	P–Si	17	87	**96**

containing coal ashes and P-containing sewage–sludge ashes.[16a–d] The effect of Fe_3O_4 was unique: it greatly decreased the tensile strength of P–Si but did not affect those of Na–Si and K–Si, suggesting strong interaction between P and Fe.[42b] These results provide basic information on the chemical effects of additives, and this information is useful for developing additives that can be used in commercial plants. Controlling the physical effects (*i.e.*, the porosity of the powder bed) is also an important function of additives.[16a,b] Increasing the porosity of the powder bed (*i.e.*, forming a poorly packed powder bed) was also found to decrease tensile strength. This effect was particularly remarkable for real ash with various causes of adhesion. To increase porosity, nanoparticles with low packing ability and additives that can form voids in the powder bed by gas release (*e.g.*, Al salts) were effective.[58]

Conclusions

Studies using real ash have contributed to understanding of the behaviour occurring in commercial plants and have suggested the potential impact of ash chemistry on adhesion. Meanwhile, synthetic ash with well-designed chemical characteristics enables a mechanistic understanding of the impact of ash chemistry on adhesion.

This review focused on two types of synthetic ash. The first was based on the concept of synthetic ash that simulated simplified real ash. Studies involving such synthetic ash have provided important insights, such as the effects of various factors (*e.g.*, the SiO_2/Al_2O_3 ratio, the CaO content and the Fe_2O_3 content) on the adhesion behaviour of real ash. However, although these studies attempted to simulate real ash, the types of behaviour exhibited by real ash remain difficult to explain, reflecting the complexity of ash chemistry. The second type of synthetic ash that has been studied comprises simple systems consisting of only 2–3 elements (components), which do no attempt to duplicate real ash. Studies on this type of ash have contributed to understanding the effects of specific elements (*e.g.*, Na, K, and P) or specific interactions (*e.g.*, P-related interactions) on particle adhesion. This provides a mechanistic understanding of the behaviour that can occur in real ash.

Fully understanding the behaviour of real ash on the basis of the results for individual synthetic ash explained in this review is difficult. However, each finding is an important piece in understanding the adhesion. As research on synthetic ash progresses, a large number of datasets will be collected, which will be useful for understanding the phenomena of real ash.

Conflicts of interest

There are no conflicts to declare.

Data availability

No primary research results, software or code have been included and no new data were generated or analysed as part of this review.

Acknowledgements

The authors would like to express sincere gratitude to Prof. Dr Hidehiro Kamiya and other collaborators for their contributions.

Notes and references

1 (*a*) F. Sher, S. Hameed, N. S. Omerbegović, A. Chupin, I. U. Hai, B. Wang, Y. H. Teoh and M. J. Yildiz, *Energy Convers. Manage.*, 2025, **323**, 119213; (*b*) Y. Shen, *Int. J. Hydrogen Energy*, 2024, **66**, 90–102; (*c*) C. Fushimi, *Energy Fuels*, 2021, **35**, 3715–3730.

2 (*a*) F. Wang, W. Peng, X. Zeng, D. Sun, G. Cui, Z. Han, C. Wang and G. Xu, *Sci. Total Environ.*, 2024, **953**, 175954; (*b*) R. Mishra, C.-M. Shu, A. R. K. Gollakota and S.-Y. Pan, *Energy Convers. Manage.*, 2024, **321**, 118997.

3 (*a*) C. T. Alves, J. A. Onwudili, P. Ghorbannezhad and S. Kumagai, *Sustainable Energy Fuels*, 2023, **7**, 3505–3540; (*b*) D. Lee, H. Nam, M. W. Seo, S. H. Lee, D. Tokmurzin, S. Wang and Y.-K. Park, *Chem. Eng. J.*, 2022, **447**, 137501; (*c*) J. Ren, Y.-L. Liu, X.-Y. Zhao and J.-P. Cao, *J. Energy Inst.*, 2020, **93**, 1083–1098.

4 (*a*) K. J. Abioye, N. Y. Harun, S. Sufian, M. Yusuf, A. H. Jagaba, B. C. Ekeoma, H. Kamyab, S. Sikiru, S. Waqas and H. Ibrahim, *J. Energy Inst.*, 2024, **112**, 101490; (*b*) D. Yu, X. Yu, J. Wu, J. Han, F. Liu and H. Pan, *Energy Fuels*, 2021, **35**, 17241–17260; (*c*) J. Zhai, I. T. Burke and D. I. Stewart, Beneficial management of biomass combustion ashes, *Renewable Sustainable Energy Rev.*, 2021, **151**, 111555.

5 J. Yu, Q. Guo, Y. Gong, L. Ding, J. Wang and G. Yu, *Fuel Process. Technol.*, 2021, **214**, 106723.
6 S. Donatello, D. Tong and C. R. Cheeseman, *Waste Manage.*, 2010, **30**, 1634–1642.
7 (*a*) U. Kleinhans, C. Wieland, F. J. Frandsen and H. Spliethoff, *Prog. Energy Combust. Sci.*, 2018, **68**, 65–168; (*b*) Z. He, J. Cao and X. Zhao, *Energy Fuels*, 2022, **36**, 8925–8947; (*c*) Y. Niu, H. Tan and S. Hui, *Prog. Energy Combust. Sci.*, 2016, **52**, 1–61.
8 (*a*) J. D. Morris, S. S. Daood, S. Chilton and W. Nimmo, *Fuel*, 2018, **230**, 452–473; (*b*) J. Shabanian and J. Chaouki, *Chem. Eng. J.*, 2017, **313**, 580–590.
9 J.-W. Zhao, H.-Y. Wang, L. Feng, J.-Z. Zhu, J.-X. Liu and W.-X. Li, *Chem. Rev.*, 2024, **124**, 164–209.
10 (*a*) S. V. Vassilev, D. Baxter, L. K. Andersen, C. G. Vassileva and T. J. Morgan, *Fuel*, 2012, **94**, 1–33; (*b*) S. V. Vassilev, C. G. Vassileva, Y.-C. Song, W.-Y. Li and J. Feng, *Fuel*, 2017, **208**, 377–409; (*c*) B. Chen, P. Perumal, M. Illikainen and G. Ye, *J. Build. Eng.*, 2023, **71**, 106386; (*d*) C. Tang, W. Pan, J. Zhang, W. Wang and X. Sun, *Fuel*, 2022, **316**, 123269; (*e*) M. Tanyıldızı, V. E. Uz and İ. Gökalp, *Constr. Build. Mater.*, 2023, **398**, 132435.
11 R. Karyappa, P. J. Ong, J. Bu, L. Tao, Q. Zhu and C. Wang, *Fuel*, 2025, **381**, 133216.
12 (*a*) S. V. Vassilev, C. G. Vassileva and V. S. Vassilev, *Fuel*, 2015, **158**, 330–350; (*b*) N. Gao, K. Kamran, C. Quan and P. T. Williams, *Prog. Energy Combust. Sci.*, 2020, **79**, 100843.
13 F. Di Capua, S. de Sario, A. Ferraro, A. Petrella, M. Race, F. Pirozzi, U. Fratino and D. Spasiano, *Sci. Total Environ.*, 2022, **823**, 153750.
14 (*a*) S. Zhou, C. Liu and L. Zhang, *Energy Fuels*, 2020, **34**, 1–15; (*b*) W. Ma, T. Wenga, F. J. Frandsen, B. Yan and G. Chen, *Prog. Energy Combust. Sci.*, 2020, **76**, 100789.
15 S. He, A. Bijl, L. Rohrbach, Q. Yuan, D. S. Santosa, Z. Wang, H. J. Heeres and G. Brem, *Chem. Eng. J.*, 2021, **420**, 129714.
16 (*a*) G. Horiguchi, R. Fujii, Y. Yamauchi, H. Okabe, M. Tsukada, Y. Okada and H. Kamiya, *Energy Fuels*, 2018, **32**, 13015–13020; (*b*) M. Ito, G. Horiguchi, T. Hariu, A. Ito, H. Kamiya and Y. Okada, *Powder Technol.*, 2020, **374**, 492–495; (*c*) G. Horiguchi, M. Ito, A. Ito, H. Kamiya and Y. Okada, *Fuel*, 2022, **321**, 124110; (*d*) J. Gao, M. Matsushita, G. Horiguchi, R. Fujii, M. Tsukada, Y. Okada and H. Kamiya, *Energy Fuels*, 2019, **33**, 9363–9366; (*e*) M. Tsukada, H. Yamada and H. Kamiya, *Adv. Powder Technol.*, 2003, **14**, 707–717; (*f*) Y. Shao, N. Aoki, Z. Tong, W. Zhong, A. Yu and H. Kamiya, *Adv. Powder Technol.*, 2016, **27**, 215–222; (*g*) M. Tsukada, K. Kawashima, H. Yamada, Y. Yao and H. Kamiya, *Powder Technol.*, 2008, **180**, 259–264.
17 (*a*) E. Atallah, F. Defoort, A. Pisch and C. Dupont, *Fuel Process. Technol.*, 2022, **235**, 107369; (*b*) E. Jak, *Fuel*, 2002, **81**, 1655–1668.
18 (*a*) K. Matsuoka, T. Yamashita, K. Kuramoto, Y. Suzuki, A. Takaya and A. Tomita, *Fuel*, 2008, **87**, 885–893; (*b*) S. F. Miller and H. H. Schobert, *Energy Fuels*, 1994, **8**, 1197–1207.
19 (*a*) L. Zhang, X. Song, Y. Li, J. Wei, Y. Bai, J. Wang, P. Lv, W. Su, G. Xu and G. Yu, *Energy Fuels*, 2024, **38**, 4769–4786; (*b*) Y. Liu, K. Yin, J. Wu, D. Mei, J. Konttinen, T. Joronen, Z. Hu and C. He, *Chem. Eng. J.*, 2023, **478**, 147429.
20 Y. Kousaka and Y. Endo, *KONA Powder Part. J.*, 1994, **12**, 7–16.
21 H. Kamiya, A. Kimura, M. Tsukada and M. Naito, *Energy Fuels*, 2002, **16**, 457–461.
22 Y. Niu, Y. Zhu, H. Tan, S. Hui, Z. Jing and W. Xu, *Fuel Process. Technol.*, 2014, **128**, 499–508.
23 D. Yu, Z. Xue and T. Mu, *Chem. Soc. Rev.*, 2021, **50**, 8596.
24 (*a*) P. Sun, C. Wang, M. Zhang, L. Cui and Y. Dong, *Sci. Total Environ.*, 2023, **901**, 165985; (*b*) E. O. Lidman Olsson, P. Glarborg, K. Dam-Johansen and H. Wu, *Energy Fuels*, 2023, **37**, 6907–6998; (*c*) F. Li, H. Fan, X. Wang, T. Wang and Y. Fang, *Fuel*, 2019, **239**, 1338–1350; (*d*) H. Namkung, Y.-J. Lee, J.-H. Park, G.-S. Song, J. W. Choi, Y.-C. Choi, S.-J. Park and J.-G. Kim, *Fuel*, 2018, **225**, 266–276.
25 Y. I. Rabinovich, M. S. Esayanur and B. M. Moudgil, *Langmuir*, 2005, **21**, 10992–10997.
26 (*a*) Z. He, W. L. Saw, P. J. van Eyk, G. J. Nathan and P. J. Ashman, *Energy Fuels*, 2020, **34**, 3210–3222; (*b*) Z. He, W. L. Saw, P. J. van Eyk, G. J. Nathan and P. J. Ashman, *Ind. Eng. Chem. Res.*, 2020, **59**, 1712–1722; (*c*) D. Lynch, A. M. Henihan, W. Kwapinski, L. Zhang and J. J. Leahy, *Energy Fuels*, 2013, **27**, 4684–4694.
27 (*a*) S. Z. Ajabshir, D. Barletta and M. Poletto, *KONA Powder Part. J.*, 2025, **42**, 100–120; (*b*) H. Lu, J. Cao, X. Guo, X. Gong and C. Luo, *Chem. Eng. Res. Des.*, 2020, **160**, 1–10; (*c*) M. J. Espin, J. M. P. Ebri and J. M. Valverde, *Chem. Eng. J.*, 2019, **378**, 122166.
28 (*a*) Z. Yang, F. Li, M. Ma, H. Fan, X. Liu and Y. Fang, *J. Environ. Chem. Eng.*, 2024, **12**, 112863; (*b*) H. Hariana, H. Ghazidin, A. Darmawan, E. Hilmawan, Prabowo and M. Aziz, *Bioresour. Technol. Rep.*, 2023, **23**, 101531; (*c*) M. Zhai, X. Li, D. Yang, Z. Ma and P. Dong, *J. Cleaner Prod.*, 2022, **336**, 130361.
29 (*a*) L. A. Hansen, F. J. Frandsen, K. Dam-Johansen and H. S. Sørensen, *Thermochim. Acta*, 1999, **326**, 105–117; (*b*) W. Shi, J. Bai, L. Kong, H. Li, Z. Bai, S. V. Vassilev and W. Li, *Fuel*, 2021, **287**, 119537; (*c*) Y. Li, J. Zhang, G. Wang, J. Qiao, P. Wang and W. Liang, *Energy Sci. Eng.*, 2019, **7**, 3332–3343.
30 (*a*) Y. Wang, B. Liang, Y. Liang, W. Fan, J. Liu, S. Niu and K. Han, *J. Energy Inst.*, 2025, **118**, 101921; (*b*) Y. Lv, Y. Lei, S. Hui, Y. Li and Y. Niu, *Fuel*, 2024, **364**, 131049; (*c*) R. Weber, Y. Poyraz, M. Mancini and A. Schwabauer, *Fuel*, 2021, **290**, 120033.
31 V. Francia, L. A. A. Yahia, R. Ocone and A. Ozel, *KONA Powder Part. J.*, 2021, **38**, 3–25.
32 H. Rumpf, *Chem. Ing. Tech.*, 1970, **42**, 538–540.
33 (*a*) P. García-Triñanes, S. Luding and H. Shi, *Adv. Powder Technol.*, 2019, **30**, 2868–2880; (*b*) M. Ueda, Y. Shimada and S. Matsusaka, *Adv. Powder Technol.*, 2022, **33**, 103713.
34 H. Kamiya, A. Kimura, T. Yokoyama, M. Naito and G. Jimbo, *Powder Technol.*, 2002, **127**, 239–245.

35 (*a*) Y. Laxminarayan, A. B. Nair, P. A. Jensen, H. Wu, F. J. Frandsen, B. Sander and P. Glarborg, *Energy Fuels*, 2018, **32**, 4432–4441; (*b*) Y. Laxminarayan, P. A. Jensen, H. Wu, F. J. Frandsen, B. Sander and P. Glarborg, *Energy Fuels*, 2017, **31**, 8733–8741.

36 (*a*) N. Aoki, Y. Okada and H. Kamiya, *ACS Sustainable Chem. Eng.*, 2020, **8**, 18864–18868; (*b*) N. Aoki, G. Horiguchi, H. Kamiya and Y. Okada, *Ind. Eng. Chem. Res.*, 2022, **61**, 3358–3364.

37 (*a*) S. V. Vassilev, K. Kitano, S. Takeda and T. Tsurue, *Fuel Process. Technol.*, 1995, **45**, 27–51; (*b*) S. V. Vassilev, D. Baxter and C. G. Vassileva, *Fuel*, 2014, **117**, 152–183.

38 (*a*) S. V. Vassilev, D. Baxter, L. K. Andersen and C. G. Vassileva, *Fuel*, 2010, **89**, 913–933; (*b*) S. V. Vassilev, D. Baxter, L. K. Andersen and C. G. Vassileva, *Fuel*, 2013, **105**, 40–76.

39 (*a*) S. V. Vassilev and C. G. Vassileva, *Fuel*, 2007, **86**, 1490–1512; (*b*) S. V. Vassilev and C. G. Vassileva, *Fuel*, 2009, **88**, 235–245.

40 J. Lachman, M. Baláš, M. Lisý, H. Lisá, P. Milčák and P. Elbl, *Fuel Process. Technol.*, 2021, **217**, 106804.

41 M. Ito, K. Tone, G. Horiguchi, T. Koseki, H. Kamiya and Y. Okada, *J. Energy Inst.*, 2024, **115**, 101691.

42 (*a*) G. Horiguchi, T. Okuizumi, H. Kamiya and Y. Okada, *ACS Sustainable Chem. Eng.*, 2024, **12**, 4655–4661; (*b*) G. Horiguchi, M. Ito, A. Ito, H. Kamiya and Y. Okada, *ACS Sustain. Chem. Eng.*, 2021, **9**, 15315–15321; (*c*) G. Horiguchi, Y. Beppu, K. Yoshinaga, H. Kamiya and Y. Okada, *ACS Sustain. Chem. Eng.*, 2021, **9**, 3727–3734; (*d*) G. Horiguchi, R. Fujii, Y. Beppu, H. Kamiya and Y. Okada, *Ind. Eng. Chem. Res.*, 2020, **59**, 16185–16190.

43 (*a*) G. W. Bryant, G. J. Browning, H. Emanuel, S. K. Gupta, R. P. Gupta, J. A. Lucas and T. F. Wall, *Energy Fuels*, 2000, **14**, 316–325; (*b*) X. Dai, J. He, J. Bai, Q. Huang, X. Wen, L. Xie, K. Luo, J. Zhang, W. Li and S. Du, *Energy Fuels*, 2016, **30**, 2407–2413.

44 (*a*) J. Niemi, D. Lindberg, M. Engblom and M. Hupa, *Chem. Eng. Sci.*, 2017, **173**, 196–207; (*b*) L. Zhang, J. Wang, J. Wei, Y. Bai, X. Song, G. Xu, Y. Pan and G. Yu, *Energy Fuels*, 2021, **35**, 425–432.

45 (*a*) Y. Wang, Y. Xiang, D. Wang, C. Dong, Y. Yang, X. Xiao, Q. Lu and Y. Zhao, *Energy Fuels*, 2016, **30**, 1437–1444; (*b*) X.-D. Chen, L.-X. Kong, J. Bai, Z.-Q. Bai and W. Li, *Fuel*, 2017, **202**, 175–183.

46 B. Liu, Q. He, Z. Jiang, R. Xu and B. Hu, *Fuel*, 2013, **105**, 293–300.

47 (*a*) T. Yan, J. Bai, L. Kong, Z. Bai, W. Li and J. Xu, *Fuel*, 2017, **193**, 275–283; (*b*) W.-J. Shi, L.-X. Kong, J. Bai, J. Xu, W.-C. Li, Z.-Q. Bai and W. Li, *Fuel Process. Technol.*, 2018, **181**, 18–24; (*c*) C. He, J. Bai, L. Kong, X. Li, J. Guo, Z. Bai, Y. Qin and W. Li, *Fuel*, 2022, **310**, 122340; (*d*) T. Yan, L. Kong, J. Bai, Z. Bai and W. Li, *Chem. Eng. Sci.*, 2016, **147**, 74–82; (*e*) C. He, J. Bai, A. Ilyushechkin, H. Zhao, L. Kong, H. Li, Z. Bai, Z. Guo and W. Li, *Fuel*, 2019, **253**, 1465–1472.

48 W. J. Song, L. H. Tang, X. D. Zhu, Y. Q. Wu, Z. B. Zhu and S. Koyama, *Energy Fuels*, 2010, **24**, 182–189.

49 Z.-S. Yuan, J. Wang, L. Kong, J. Bai, Z. Ni, H. Li, Z. Bai and W. Li, *Fuel Process. Technol.*, 2021, **211**, 106593.

50 H. Wu, X. Liu, X. Cao, Q. Guo and G. Yu, *Fuel*, 2024, **361**, 130698.

51 (*a*) R. Balint, M. Engblom, J. Niemi, M. Hupa and L. Hupa, *Fuel*, 2024, **359**, 130386; (*b*) J. Niemi, R. Balint, M. Engblom, J. Lehmusto and D. Lindberg, *Energy Fuels*, 2019, **33**, 5883–5892; (*c*) D. Lindberg, J. Niemi, M. Engblom, P. Yrjas, T. Laurén and M. Hupa, *Fuel Process. Technol.*, 2016, **141**, 285–298.

52 (*a*) R. Faust, K. Fürsatz, P. Aonsamang, M. Sandberg, M. Kuba, N. Skoglund and P. Knutsson, *Fuel*, 2023, **331**, 125595; (*b*) C. Sevonius, P. Yrjas, D. Lindberg and L. Hupa, *Fuel*, 2020, **268**, 117300; (*c*) P. Billen, B. Creemers, J. Costa, J. V. Caneghem and C. Vandecasteele, *Biomass Bioenergy*, 2014, **69**, 71–79.

53 J. C. Park, H. Namkung, S.-P. Yoon, H. S. Seo, L.-H. Xu and H.-T. Kim, *J. Energy Inst.*, 2020, **93**, 2399–2408.

54 (*a*) Z. Yu, J. Jin, F. Hou, Y. Zhang, G. Wang, B. Liu and Z. Zhai, *Fuel*, 2021, **287**, 119462; (*b*) A. Szydełko, W. Ferens and W. Rybak, *Waste Manage.*, 2022, **150**, 161–173.

55 (*a*) G. Horiguchi, T. Fujimoto, N. Konakahara, H. Kamiya and Y. Okada, *Adv. Powder Technol.*, 2025, **36**, 104872; (*b*) T. Fujimoto, G. Horiguchi, H. Kamiya and Y. Okada, *Powder Technol.*, 2024, **444**, 120008; (*c*) G. Horiguchi, T. Fujimoto, K. Yoshinaga, Y. Okada and H. Kamiya, *Powder Technol.*, 2022, **405**, 117514; (*d*) G. Horiguchi, H. Kamiya and P. García-Triñanes, *Adv. Powder Technol.*, 2021, **32**, 283–289.

56 (*a*) J. L. Míguez, J. Porteiro, F. Behrendt, D. Blanco, D. Patiño and A. Dieguez-Alon, *Renewable Sustainable Energy Rev.*, 2021, **141**, 110502; (*b*) T. Bankefa, J. Nasah, D. Laudal and N. Andraju, *Energy Fuels*, 2024, **38**, 8460–8480; (*c*) Z. Liu, J. Jin, L. Zheng, R. Zhang, Y. Wang, X. He, S. Kong and Z. Zhai, *Fuel*, 2022, **323**, 124342; (*d*) Z. Liu, J. Jin, L. Zheng, R. Zhang, B. Dong, G. Liang and Z. Zhai, *Energy*, 2023, **262**, 125320.

57 Y. Liua, Z. Wang, Y. Lv, K. Wan, Y. He, J. Xia and K. Cen, *Fuel*, 2018, **212**, 498–505.

58 T. Okuizumi, G. Horiguchi, H. Kamiya and Y. Okada, *Energy Fuels*, 2024, **38**, 2319–2326.